A Dynamic Fracture Simulation Based on Embedded Finite Element Methods

by

Bingxiao Zhao

Department of Mechanical Engineering and Materials Science
Duke University

Date:_____

Approved:

_____
John Dolbow, Supervisor

_____
Earl Dowell

_____
Thomas Witelski

Thesis submitted in partial fulfillment of
the requirements for the degree of Master of Science in the Department of
Mechanical Engineering and Materials Science in the Graduate School of
Duke University

2012

ABSTRACT

A Dynamic Fracture Simulation Based on Embedded Finite Element Methods

by

Bingxiao Zhao

Department of Mechanical Engineering and Materials Science
Duke University

Date:_____

Approved:

_____
John Dolbow, Supervisor

_____
Earl Dowell

_____
Thomas Witelski

An abstract of a thesis submitted in partial fulfillment of
the requirements for the degreeof Master of Science in the Department of
Mechanical Engineering and Materials Science in the Graduate School of
Duke University

2012

Abstract

In this thesis, a hybrid numerical approach is proposed for modeling dynamic fracture in brittle materials. This method is based on a combination of embedded finite element methods and extrinsic cohesive zone models. The effect of different methods to enforce the kinematics at the embedded interface for crack initiation and propagation are investigated and numerically compared. Finally, Nitsche's method is suggested within the hybrid numerical schemes to simulate dynamic fracture. In the pre-failure stage, terms for consistency and stabilization are introduced into the finite element framework with Nitsche's method. When the fracture criterion is met, the extrinsic cohesive law governs the behavior of the opening surfaces by a simple change of framework without modifications of the mesh. This traction and separation law is directly implemented at the interfacial integration points through an interface approach. Upon closure of the crack surfaces in compression, Nitsche's method is suggested to weakly enforce contact conditions at crack surfaces.

The applicability of the proposed hybrid method is investigated in numerical examples. By using Nitsche's method, the main advantage of the hybrid method for modeling dynamic crack propagation is to avoid unphysical initial slopes in the numerical implementation of extrinsic cohesive laws, which affords us more accurate

crack initiation than with the penalty method. Another advantage is that the consistency and stability in the unfractured interfaces during crack propagation are maintained and hence the issues caused by the penalty method in explicit dynamic schemes are avoided. Importantly, Nitsche's method performs better than the penalty method conventionally used to prevent interpenetration under compressive loadings.

Content

Abstract iv

Content vi

List of Figures viii

Acknowledgements x

1. Introduction 1

1.1 Extrinsic CZMs and Intrinsic CZMs 1

1.2 Numerical representations of CZMs 3

1.2.1 Cohesive element approach 3

1.2.2 Discontinuous Galerkin methods/CZMs 5

1.2.3 Extended finite element methods/CZMs 6

1.2.4 Embedded finite element methods/CZMs 6

2. Numerical schemes based on embedded finite element methods/CZMs 9

2.1 Model description 9

2.2 Variational formulations in the pre – failure stage 11

2.2.1 Lagrange multiplier approach 11

2.2.2 Penalty method 12

2.2.3 Nitsche's method 14

2.3 Variational formulations in the post – failure stage 16
2.3.1 Ortiz and Pandolfi's CZM 16
2.3.2 Numerical representation of extrinsic CZMs 18
2.4 A hybrid framework for the model problem 19
2.5 Spatial discretization approach 20
2.5.1 Discrete formulation based on embedded finite element methods 23
2.5.2 Evaluation of the stabilization parameters 26
2.6 Temporary discretization 27
2.6.1 Integration schemes 28
2.6.2 Stability analysis 29
3. Numerical examples 33
3.1 Wave propagation test 34
3.2 Dynamic crack propagation 39
3.2.1 Implemental aspects of the extrinsic CZM 41
3.2.2 Crack propagation only in tension 43
3.2.3 Crack propagation in tension and compression 46
4. Conclusions 50
References 52

List of Figures

Figure 1: Representation of cohesive zone concept (a) and cohesive law (b) 2

Figure 2: Comparison of intrinsic and extrinsic CZMs: (a) bilinear intrinsic cohesive law in pure tension and pure shear (b) initially rigid extrinsic cohesive law in pure tension and pure shear 3

Figure 3: Relationship between normalized traction and normalized opening in Ortiz and Pandolfi's CZM 18

Figure 4: Representation of embedded interfaces 21

Figure 5: Discretized subdomains with overlap at the interface 22

Figure 6: Overlapping element formulation for a triangle element cut by an embedded interface. Black circles are the physical nodes generalized in the background mesh and the hollow circles are the sibling nodes. The blue nodes represent the discretization of the embedded interface in each partial element. 22

Figure 7: Illustration in 1D case for the interface position: the black nodes are physical nodes of background mesh and hollow nodes are siblings. The blue ones represent the embedded interface. The position of the interface is defined by a distance from the interface node to the physical node. 32

Figure 8: Geometry model and loading conditions in wave propagation tests 34

Figure 9: Interfacial tractions at the embedded interface with variation of different penalty parameters where k = log10 (α /E) 36

Figure 10: Interfacial tractions at the embedded interface with variation of different penalty parameters where k = log10 (α /E) 37

Figure 11: Comparison of interfacial tractions at the embedded interface with different embedded methods 38

Figure 12: Variation of critical time steps with increasing penalty parameters 39

Figure 13: Geometry model and loading conditions in dynamic crack propagation 39

Figure 14: Implemented an extrinsic linear cohesive law based on different penalty parameters.....44

Figure 15: Implemented an extrinsic cohesive law with Nitsche's method 45

Figure 16: Comparison of Penalty method and Nitsche's method in implementation of an extrinsic cohesive law 46

Figure 17: Comparison of Penalty method (k=5) and Nitsche's methods in compression for preventing interpenetrations.....47

Figure 18: Stress and Displacement field at different times.....49

Acknowledgements

First, I would like to thank my advisor, Dr. John Dolbow. Your kindness, help, support and dedication to me were invaluable. Your academic adventure and research experience enhances my interests in this field. Your consistent encouragement keeps me being energetic every day.

I also would like to thank those professors who have contributed to my better understanding of this research: Dr. Earl Dowell and Dr. Thomas Witelski. In addition, a special thank you to my great fellow, Chandrasekhar Annavarapu, who was always available there and willing to help me in difficulties. I cherish my experience in DCML spent with all my labmates: Anand Embar, Temesgen Kindo, Wen Jiang, Ziyu Zhang, Yan Feng, Mark Merewether, Curtis Lee, Andrew Stershic, Alex Kelly, Martin Hautefeuille and Justin Pogacnik.

I wish to dedicate this thesis to my parents. Thanks for having provided me such a fantastic environment for growing up and studies. Your love and support give me courage and confidence to go wherever I desire.

1. Introduction

The cohesive zone approach to model static and dynamic fracture mechanics has been widely used in simulations of crack propagation along either predefined paths or arbitrary paths by incorporating a cohesive zone model (CZM) in finite element methods to characterize the fracture process. Although the basic cohesive zone concept had been proposed by Barenblatt (1959, 1962), the cohesive zone models were adopted into numerical schemes with the development of modern numerical simulation techniques. This approach allows simulating fracture processes which occurs spontaneously rather than being specified ad hoc or a priori (Brian N. Cox, 2005). The concept of 'cohesive failure' is shown in Figure 1(Zhang, 2005). Due to the material softening from voids and micro cracks in the vicinity of the crack tip, the cohesive view is captured by surface constitutive relationships that describe the evolution of tractions generated opposite to a crack surface as a function of the jump displacement across the surfaces (K. Ravi-Chandar, 1997). These traction-separation relationships are also named cohesive laws.

1.1 Extrinsic CZMs and Intrinsic CZMs

Various cohesive zone models have been proposed for the simulation of crack propagation. The intrinsic CZMs (Xu and Needleman, 1995) incorporate with an initial slope in the traction-separation curve, which causes an artificial reduction of the stiffness. The other noteworthy models are extrinsic CZMs (Ortiz,1996) that eliminate the artificial

compliance mentioned above with a monotonically deceasing cohesive strength, although extrinsic models may lead to time-discontinuous numerical results (Papoulia KD, 2003). Their advantages, disadvantages and limitations were discussed in the literature (Zavattieri, 2001and Pandolfi, 2002). The main distinction between intrinsic and extrinsic CZMs lies in the crack initiation criteria. Intrinsic models assume that the interfacial traction firstly increases with the increasing separation until it reaches a maximum value and then decreases and finally vanishes at a critical separation value. However, the extrinsic CZMs assume that the separation only initiates when the traction reaches the maximum value. Once the separation occurs, the interfacial traction monotonically decreases as separation increases (Zhang, 2005). Ideally in extrinsic models, the initial interfacial stiffness should be infinite and the cohesive interface should not deform prior to crack propagation. In addition, since these extrinsic models require an external fracture criterion to the cohesive law during implementation, they are referred to as 'extrinsic'. See Figure 2 (Zhang, 2007). Based on the above evaluation of the two types of CZMs, it is necessary to use extrinsic CZMs for brittle fracture.

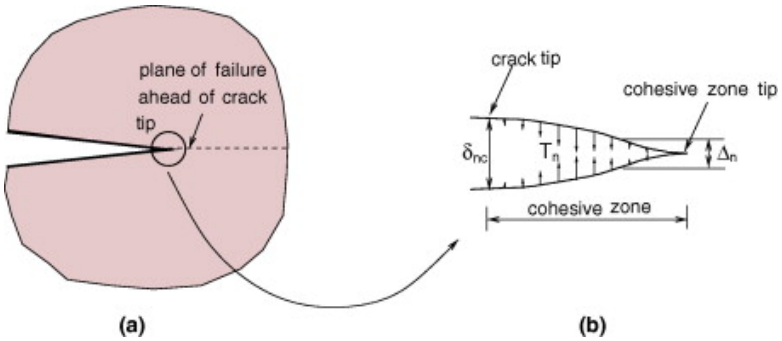

Figure 1: Representation of cohesive zone concept (a) and cohesive law (b)

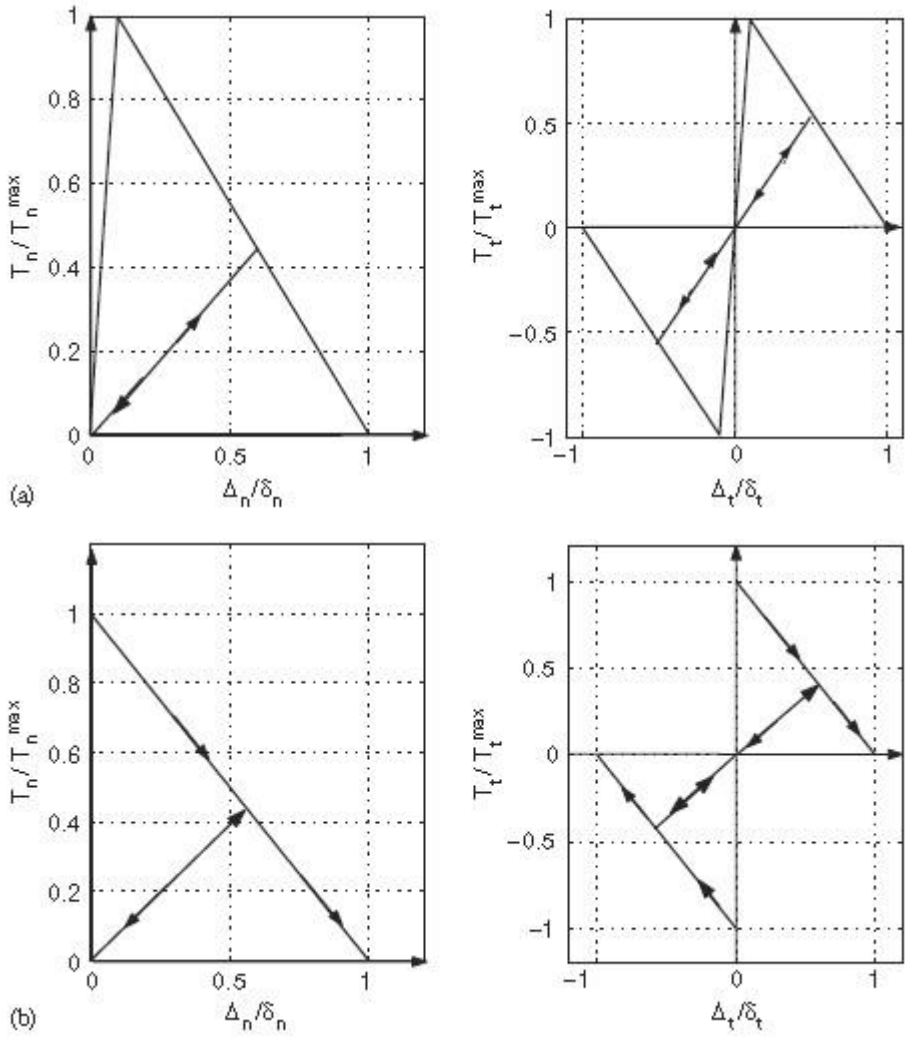

Figure 2: Comparison of intrinsic and extrinsic CZMs: (a) bilinear intrinsic cohesive law in pure tension and pure shear (b) initially rigid extrinsic cohesive law in pure tension and pure shear

1.2 Numerical representations of CZMs

1.2.1 Cohesive element approach

For numerical simulation techniques in the representation of CZMs, the most important development in computational fracture mechanics is the introduction of

cohesive element approach in the last decade. There are two ways of inserting cohesive elements between bulk elements. In the intrinsic CZMs developed by Xu and Needleman (1994), the cohesive elements are inserted at the beginning of the simulation, which makes the stage of pre-fracture taken into consideration and intrinsic cohesive law used to govern the behavior of the crack surfaces. The pre-fracture is related to the initial slope in the intrinsic cohesive law. The limits include that the crack path must be well-known in advance and the initial slope must tend to infinite in order to correctly simulate wave propagation and avoid the 'artificial compliance' which may result in a significant reduction of stiffness. Some intrinsic difficulties associated with the original formulations have been further stated by Klein (2001), such as the mesh dependence in the direction of cracks. In the extrinsic case developed by Ortiz (1996), the failure criterion based on tractions is external to cohesive elements and the extrinsic cohesive zone model is governed by a monotonically decreasing traction-separation relationship. There is no modification of the stiffness and no alteration of wave propagation during the pre-fracture stage. However, the insertion of cohesive elements with an extrinsic model still requires complex topological data structures due to the mesh updating in dynamic problems (Zhang and Paulino, 2007). Parallel computing is helpful in cohesive element methods based on mesh refinements (Becker and Noels, 2011) and the extension to parallel simulations and further difficulties on propagating topological changes in the mesh across processor boundaries are the main issues. In response to the above difficulties, new approaches for dynamic crack propagation have been developed.

1.2.2 Discontinuous Galerkin methods/CZMs

Discontinuous Galerkin methods are now commonly used to solve hyperbolic problems and elliptic problems. This method allows weakly enforcing the compatibility condition through element boundary integral terms, which can be directly used to model fracture problem since the interface elements are naturally present. This so-called interface approach for crack propagation simulations is proposed by Mergheim (2004) and further investigated by Seagraves and Radovitzky (2009, 2010). It has been shown that the interface approach based on DG is scalable when parallelized (Radovitzky, 2009) and does not require the use of complex topological information when being implemented easily into existing finite element codes(Becker and Noels, 2011). The recent contribution of this approach aims at using Nitsche's method which can be seen as the origin of discontinuous Galerkin methods to weakly enforce the perfect continuity at interfaces instead of using the penalty method in the pre-failure region. Nitsche (1970) originally introduced a method to weakly enforce Dirichlet boundary conditions, then Douglas and Dupont (1976) extended it into the weak enforcement of the continuity of solutions at the interior boundaries. More details about DG methods can be seen in Cockburn's book (2000). This hybrid DG/ CZMs approach also belong to interelement crack methods, since the crack is modeled by separations along element edges that are mechanically bounded by cohesive laws.

1.2.3 Extended finite element methods/CZMs

Contrary to the interelement crack approaches, alternative approaches for modeling dynamic crack propagation are based on the extended finite element method (X-FEM) which allows cracks of arbitrary geometry within elements without remeshing, rather than only along element edges. The essential idea in the formulation of the XFEM is that the displacement field incorporates the enriched discontinuity as additional terms in the displacement approximation (Moes, Dolbowand Belytschko, 1999). It is characterized by the consideration of adding enrichments to the classical finite element approximation space to describe inner-element discontinuities and singularities. The XFEM was first used to simulate dynamic crack propagation by Belytschko (2003). Later, Song (2006) combined the discretization approach proposed by Hansbo and Hansbo (2004) which uses the same basic functions. Then some work to study the stability of the explicit dynamic schemes and energy conservation has been done by Rethore (2004, 2005). Based on the basic ideas in XFEM, Remmers (2003) introduced cohesive segments methods for dynamic crack propagation in brittle materials, which can be seen as a variant of XFEM where a crack is initiated by inserting discontinuities that spans three elements per time. A recent review on XFEM is given by Fries and Belytschko (2010).

1.2.4 Embedded finite element methods/CZMs

Recently within the XFEM, an efficient embedded finite element method based on Nitsche's method to weakly enforce constraints at interfaces was developed for steady problems (Dolbow and Harari, 2009). As for the consideration of embedded

interfaces, the key idea behind the method is a local enhancement of the kinematics where the finite element mesh is not aligned with the interface geometry. Nitsche based stabilization parameter was originally freely defined in the work of Hansbo and Hansbo (2004). Dolbow and Harari proposed an analytical formulation to determine the Nitsche based stabilization parameters at an element level, which resulted in a more robust computational algorithm for interface problems. Later, various strategies to enforce kinematics at an embedded interface for transient problems and the effect of spatial stabilization on the temporal stability of explicit dynamic schemes with interfacial constraints were further investigated by Annavarapu et al. (2012). Thus, this robust embedded finite element method is now particularly efficient for the problems where an interface evolves in time or has complex microstructural geometrical shapes, which highlights the future for modeling dynamic fracture in brittle materials with micro crack propagation. In addition, since interfaces are naturally introduced within elements based on Hansbo's formulation, the interface approach for modeling post-failure stage originally proposed with Discontinuous Galerkin methods may also work here.

Therefore, by combining a linear extrinsic CZM to describe the fracture mechanism in brittle materials, the performance of embedded interface algorithms for dynamic fracture simulations would be investigated in the following chapters with the emphasis on the comparison of penalty method and Nitsche's method implemented in different stages of dynamic fracture processes.

This thesis is outlined as follows. The numerical schemes including variational forms, spatial discretization, temporal discretization and stability analysis are introduced in Chapter 2. Chapter 3 describes numerical examples which verify the numerical simulation procedures and illustrate the effects of different methods to weakly enforce interfacial constraints on the dynamic failure behavior of materials during the whole fracture processes. The work presented here focuses on two-dimensional (2-D) fracture.

2. Numerical schemes based on embedded finite element methods/CZMs

In this chapter, the pre-failure stage considered as uncracked interfaces is modeled through the embedded finite element method. It is assumed that the potential failure zone is known and introduced on an interface Γ_{int} along the potential zone. This method allows a local enhancement of kinematics on an embedded interface evolving in time or whose geometry is not aligned with the background finite element mesh. Since two-sided interfaces are naturally introduced in embedded interface algorithms, an interface approach for implementing cohesive zone models is applied to simulate the post – failure stage when the failure criterion is satisfied. Jumps of quantities across Γ_{int} here are denoted by $[\![\cdot]\!] = (\cdot)^1 - (\cdot)^2$. The constitutive law of the interface and its behavior is governed by appropriate traction-separation laws that are independent of constitutive relationships in the surrounding subdomains. To combine the interface approach with embedded finite element methods, the fraction criteria is described by a switching factor. Thus, a hybrid weak formulation is proposed for dynamic fracture problems.

Based on the hybrid weak formulation, spatial and temporal discretization approaches are introduced with an emphasis on stabilization analysis in this chapter.

2.1 Model description

An elastodynamic problem considered here is defined on the whole domain Ω which is divided into two subdomains Ω^1 and Ω^2 by an embedded interface Γ_{int}. On the

Dirichlet boundaries Γ_d^m as part of the exterior boundaries, the displacements are specified as $u_i^m = u_d^m$. On the Neumann boundaries Γ_n^m, the tractions are specified as $\sigma_{ij}^m n_j^m = h_i^m$ where m = 1, 2 is an index denoting the subdomain Ω^m. The rest of the exterior boundary is assumed to be traction free. The governing equations of an elastodynamic problem are given by:

$$\sigma_{ij,j}^m = \rho^m \ddot{u}_i^m \quad in\ \Omega = \{\Omega^1 \cup \Omega^2\} \times (0,T)$$

$$u_i^m = u_d^m \quad on\ \Gamma_d = \{\Gamma_d^1 \cup \Gamma_d^2\} \times (0,T)$$

$$\sigma_{ij}^m n_j^m = h_i^m \quad on\ \Gamma_n = \{\Gamma_n^1 \cup \Gamma_n^2\} \times (0,T)$$

$$u_i^m(0) = u_0^m \quad in\ \Omega = \{\Omega^1 \cup \Omega^2\}\ at\ T = 0$$

$$\dot{u}_i^m(0) = \dot{u}_0^m \quad in\ \Omega = \{\Omega^1 \cup \Omega^2\}\ at\ T = 0$$

In addition, the interfacial conditions are traction balance and displacement continuity prior to failure or in compression after complete failure:

$$\sigma_{ij}^1 n_j^1 = -\sigma_{ij}^2 n_j^2 \ \ on\ \Gamma_{int} \times (0,T)$$

$$u_i^1 = u_i^2 \ \ on\ \Gamma_{int} \times (0,T)$$

The material property in each subdomain follows a linear elastic constitutive relationship such that $\sigma_{ij}^m = C_{ijkl}^m u_{(k,l)}^m$. In tension, the behavior of the interfaces created by crack surfaces are controlled by cohesive laws depending on the jump in displacement across opened surfaces:

$$\sigma_{ij}^1 n_j^1 = -\sigma_{ij}^2 n_j^2 \quad on\ \Gamma_{int} \times (0,T)$$

$$t_i^m = f(\llbracket u^i \rrbracket) = \sigma_{ij}^m n_j^m \ \ on\ \Gamma_{int} \times (0,T)$$

At the dynamic aspects, the Lagrange energy functional of the whole dynamic system can be evaluated by the subtraction of kinetic energies and potential energies:

$$L = \sum_m \left(\frac{1}{2} \int_{\Omega^m} \dot{u}_i^m \, \rho^m \dot{u}_i^m d\Omega - \frac{1}{2} \int_{\Omega^m} u_{(i,j)}^m \, C_{ijkl}^m u_{(k,l)}^m d\Omega + \int_{\Gamma_n^m} h_i^m \, u_i^m d\Gamma \right)$$

According to Hamilton's principle, the set of governing equations can also be derived by minimizing the integral $I = \int L \, dt$ such that $\delta I = \delta(\int L \, dt) = 0$, subject to interfacial constraints on Γ_{int}. In the following, the variational formulations including interfacial kinematics are described by a constrained Lagrangian.

2.2 Variational formulations in the pre – failure stage

Define the space of solutions and variations as following:

$$U = \left\{ u_i(t) \in H^1\left(\{\Omega^1 \cup \Omega^2\} \times (0,T)\right), u_i|_{\Gamma_d} = u_d \right\}$$

$$V = \left\{ \delta u_i \in H^1(\{\Omega^1 \cup \Omega^2\}), \delta u_i|_{\Gamma_d^1 \cup \Gamma_d^2} = 0 \right\}$$

Based on energy aspects, several approaches have been used to treat interfacial constraints within a variational framework. In the following, I will further derive the variational form in the pre-failure state according to these methods to enforce perfect continuity at uncracked interfaces.

2.2.1 Lagrange multiplier approach

In this classic approach, Lagrange multipliers are used to account for interfacial constraints in a constrained minimization problem within the standard variational framework. The essential boundary condition of displacement continuity at the interface is built into the potential energy of the Lagrange energy functional as an additional constrained term. Lagrange multipliers $\lambda_i(t) \in l = H^{-1/2}\left(\Gamma_{int} \times (0,T)\right)$ are introduced into the potential energy of the system as follows:

$$L^{Lag} = L - \int_{\Gamma_{int}} \lambda_i \, [\![u_i]\!] d\Gamma$$

where, $[\![\cdot]\!]$ denotes the jump in displacement across an interface as $u_i^1 - u_i^2$. Displacement continuity is specified as $[\![u_i]\!] = 0$. The Lagrange multipliers here are interpreted as the traction at the interface. The following variational formulation, subject to the interfacial displacement continuity constraint, is obtained based on δL^{Lag}:

Find $(u_i, \lambda_i) \in U \times l$ such that for all $(\delta u_i, \delta \lambda_i) \in V \times H^{-1/2}(\Gamma_{int})$:

$$\delta I = \delta L - \int_{\Gamma_{int}} \lambda_i \, [\![\delta u_i]\!] d\Gamma - \int_{\Gamma_{int}} \delta \lambda_i \, [\![u_i]\!] d\Gamma = 0$$

$$\delta L = \sum_m \left(- \int_T \delta u_i^m \, \rho^m \ddot{u}_i^m d\Omega - \int_{\Omega^m} \delta u_{(i,j)}^m \, C_{ijkl}^m u_{(k,l)}^m d\Omega + \int_{\Gamma_n^m} h_i^m \, \delta u_i^m d\Gamma \right)$$

2.2.2 Penalty method

In the penalty method, the Dirichlet constraint at the interface is enforced in a spring-like way:

$$\sigma_{ij}^1 n_j^1 = -\sigma_{ij}^2 n_j^2 = \alpha_{ij} [\![u_i]\!]$$

where α_{ij} can be interpreted as the stiffness of a spring that connects two subdomains together. Further, we choose $\alpha_{ij} = \frac{1}{2} \alpha \delta_{ij}$. Since the displacement at the interface is double-valued, two finite element nodes have to be introduced at one material point. Particularly in the penalty method, each pair of nodes at the interface is artificially held together with the help of the penalty parameter, even though the choice of an appropriate penalty parameter is questionable at this point. The Lagrangian based on the penalty method is expressed as:

$$L^{Pen} = L - \int_{\Gamma_{int}} \frac{1}{2} [\![u_i]\!] \alpha [\![u_i]\!] d\Gamma$$

To obtain the variational formulation from the stationarity of the action integral, I obtain:

$$\delta I = \delta L - \int_{\Gamma_{int}} [\![\delta u_i]\!] \alpha [\![u_i]\!] \, d\Gamma = 0$$

It has been shown that the Dirichlet constraint would obtain a better approximation with increasing penalty parameters. Only when the penalty parameter tends to infinity, the interfacial constraints would be achieved exactly, so this method is not variationally consistent due to this particular approximation. Morever, the penalty parameter would cause a series of issues in numerical schemes. It directly affects the spectral radius of the linear operator resulting from the discrete system. Moreover, a very large penalty parameter is usually necessary to obtain accurate results, which results in an ill-conditioned system of equations. For explicit dynamic schemes, the critical time step for the temporal stability is inversely related to the maximum eigenvalue of the discrete system which is a function of the penalty parameter and even causes artificial oscillations of the interfacial tractions (Simone, 2004). Further discussion will be made about these restrictions on the choice of penalty parameters in Chapter 3. Due to the disadvantages of the penalty method, Nitsche's method is hence suggested in the hybrid method for dynamic crack propagation.

2.2.3 Nitsche's method

By adding consistency terms into penalty methods, the displacement continuity can be weakly enforced by Nitsche's method (Juntunen, 2009 and Wriggers, 2008). This method was originally introduced to enforce Dirichlet boundary conditions in a weak sense, which was later extended in the weak enforcement of the continuity at the interior boundaries. Recently, Nitsches's method is increasingly popular for embedded discontinuities in structures and materials (Dolbow and Harari, 2009) in combination with domain decomposition techniques in references (Hansbo and Hansbo, 2002).

Nitsche's method can also be derived by using an augmented Lagrange multiplier approach, where the augmented Lagrangian is defined by :

$$L^{Aug} = L - \int_{\Gamma_{int}} (\lambda_i + \frac{1}{2}[\![u_i]\!]\alpha)\,[\![u_i]\!]d\Gamma$$

To obtain variational formulation from the stationarity of the action integral, I obtain:

$$\delta I = \delta L - \int_{\Gamma_{int}} \delta\lambda_i\,[\![u_i]\!]d\Gamma - \int_{\Gamma_{int}} [\![\delta u_i]\!](\,\lambda_i + \alpha[\![u_i]\!])d\Gamma = 0$$

By applying the divergence theorem, the interfacial terms are obtained as:

$$-\sum_m \int_{\Gamma_{int}} \delta u_i^m\,\sigma_{ij}^m n_j^m d\Gamma - \int_{\Gamma_{int}} \delta\lambda_i\,[\![u_i]\!]d\Gamma - \int_{\Gamma_{int}} [\![\delta u_i]\!](\,\lambda_i + \alpha[\![u_i]\!])d\Gamma = 0$$

By using the traction continuity at the interface $\sigma_{ij}^1 n_j^1 = -\sigma_{ij}^2 n_j^2$, I further obtain:

$$-\int_{\Gamma_{int}} \delta\lambda_i\,[\![u_i]\!]d\Gamma - \int_{\Gamma_{int}} [\![\delta u_i]\!](\,\langle\sigma_{ij}\rangle_\gamma n_j^1 + \lambda_i + \alpha[\![u_i]\!])d\Gamma = 0$$

where $\langle\sigma_{ij}\rangle_\gamma = \gamma^1\sigma_{ij}^1 + \gamma^2\sigma_{ij}^2$ and $\gamma^1 + \gamma^2 = 1$, represent the weighted average of the stress on the interface. The displacement continuity constraint at the interface has been built in and also the Lagrange multiplier can be physically interpreted as the weighted average of interfacial traction such that $\lambda_i = -\langle\sigma_{ij}\rangle_\gamma n_j^1$. Thus, the variational form arrives at:

$$\delta I = \delta L + \int_{\Gamma_{int}} \langle\delta\sigma_{ij}\rangle_\gamma n_j^1 [\![u_i]\!] d\Gamma + \int_{\Gamma_{int}} [\![\delta u_i]\!]\langle\sigma_{ij}\rangle_\gamma n_j^1 \, d\Gamma - \int_{\Gamma_{int}} \alpha[\![\delta u_i]\!][\![u_i]\!] d\Gamma = 0$$

It turns out that the standard form of Nitsche's method is recovered when $\gamma^1 = \gamma^2 = 0.5$. Otherwise, it is the so-called weighted Nitsche's method that choosing γ^m belonging to (0,1) at an element level gives the flexibility to guarantee both spatial and temporal stabilization, details can be seen in Annavarapu's work (2012). These two additional integral terms account for the variational consistency and symmetry while the penalty term is only necessary for the stabilization. Dolbow and Harari (2009) have numerically analysed the choice of stabilization parameter in Nitsche's method and proposed an efficient formulation to automatically determinate the Nitsche stabilization parameters for quasi-static problems at an element level. Based on the mentioned contributions about stability concerns in quasi-static problems, usually it is natural to extend quasi-static approaches into transient problems. To model complex physical problems such as dynamic cohesive fracture, additional studies are still necessary to figure out the effect spatial stabilization has on the temporal stability of explicit dynamic

schemes. Details on the temporal stability analysis of dynamic crack propagation will be further investigated in Chapter 4.

This consistent strategy presented here is to tie interfacial finite element nodes together without using large penalty parameters to obtain the accuracy in the pre-failure stage. Since the average interfacial traction is enforced to vanish in an integral sense, the double-valued displacement fields are treated consistently. In Chapter 4, comparison has been made between penalty and Nitsche's method in wave propagation and dynamic crack propagation.

2.3 Variational formulations in the post – failure stage

The interface approach to model cohesive failure is applied to account for strong discontinuities in the displacement field along embedded interfaces, since the two- sided interface has already been generated in the embedded interface algorithms.

To characterize cohesive fracture processes, CZMs are typically used in the simulation of crack propagation. Two types of CZMs have been particularly introduced in Section 1.1 with an emphasis on advantages of extrinsic CZMs for modeling fracture in brittle materials. In the present investigation, the one adopted here is proposed by Ortiz and Pandolfi (1999), which is discussed as follows.

2.3.1 Ortiz and Pandolfi's CZM

It is described as an extrinsic initially rigid cohesive zone model, which eliminates the artificial compliance that results from the elastic deformation of cohesive interfaces in intrinsic models. As for ideal explicit CZMs, the stiffness of the initial

interfaces should be infinity. That means, the cohesive interfaces should generate no deformation prior to crack propagation. To implement the explicit CZMs, the separation is only initialized when the current interfacial traction reaches the critical fracture stress T_n^{max}, which corresponds to the infinite initial slope of the traction separation curve. Particularly by the interface approach, cohesive laws directly control the mechanical behaviors of opening embedded interfaces when an external fracture criterion is met without creating surfaces and doubling nodes any more. In addition, only the normal component of the cohesive traction is considered in this work. Thus, the fracture initiation condition is described as:

$$T_n \geq T_n^{max}$$

The traction – separation relationship is applied to govern the behavior of cohesive surfaces when the above fracture initiation condition is met. When the current separation $[\![u]\!]_n$ keeps increasing due to local loading, the cohesive traction linearly reduces to a zero value where the crack has fully developed and the critical normal opening displacement is denoted as $l_{n,cr}$. In order to capture the history point where the crack starts to close due to local unloading, the maximum separation $[\![u]\!]_{max}$ is updated during the first loading path.

$$T_n = T_n^{max}\left(1 - \frac{[\![u]\!]_n}{l_{n,cr}}\right)$$

$$[\![u]\!]_n^{max} = [\![u]\!]_n \quad when\ l_{n,cr} > [\![u]\!]_n \geq [\![u]\!]_{n-1}^{max}$$

When the crack starts to close due to local unloading after the separation reaches $[\![u]\!]_{max}$ in the history, the linear unloading relation is applied as:

$$T_n = T_n^{max} \frac{[\![u]\!]_n}{[\![u]\!]_{max}} \left(1 - \frac{[\![u]\!]_{max}}{l_{n,cr}}\right) \quad when \ [\![u]\!]_n < [\![u]\!]_{max}$$

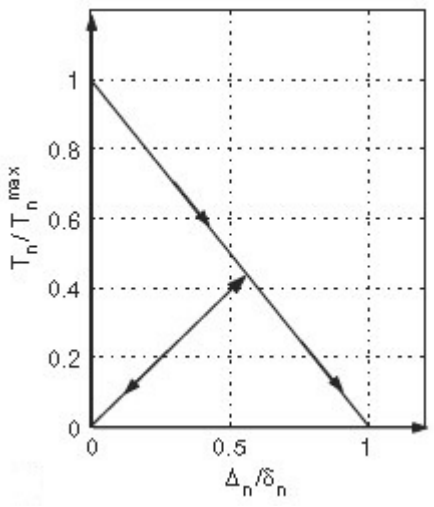

Figure 3: Relationship between normalized traction and normalized opening in Ortiz and Pandolfi's CZM

If the crack opens again after unloading, the reloading path obeys the unloading path until the current separation reaches $[\![u]\!]_{max}$ again and then follows the original loading path. The traction – separation curve in normal cases is correspondingly illustrated in Figure 3.

2.3.2 Numerical representation of extrinsic CZMs

To implement the specific cohesive law with an extrinsic CZM, the Dirichlet constraint at the interface is enforced as a function of the jump in displacement across the interface:

$$\sigma_{ij}^1 n_j^1 = -\sigma_{ij}^2 n_j^2 = f([\![u_i]\!])$$

The Lagrangian based on the interface approach is expressed as:

$$L^{Int} = L - \int_{\Gamma_{int}} [\![u_i]\!] f([\![u_i]\!]) d\Gamma$$

To obtain the variational formulation, we consider that

$$\delta I = \delta L - \int_{\Gamma_{int}} [\![\delta u_i]\!] f([\![u_i]\!])\, d\Gamma = 0$$

, where the cohesive law is weakly enforced into the variational formulation in the post – failure stage.

2.4 A hybrid framework for the model problem

Based on the last two sections, a switching factor β representing the fraction initiation condition and a switching factor μ representing the change between Nitsche's method and penalty method are introduced into the model problem in order to combine pre – failure stage and post – failure stage. Therefore, the weak formulation of this hybrid method can be written as:

Define the space of solutions and variations as:

$$U = \left\{u_i(t) \in H^1\left(\{\Omega^1 \cup \Omega^2\} \times (0,T)\right), u_i|_{\Gamma_d} = u_d\right\}$$

$$V = \left\{\delta u_i \in H^1(\{\Omega^1 \cup \Omega^2\}), \delta u_i|_{\Gamma_d^1 \cup \Gamma_d^2} = 0\right\}$$

To find $u_i \in U$such that for all $(\delta u_i) \in V$:

$$\sum_m \left(\int_T \delta u_i^m \rho^m \ddot{u}_i^m d\Omega + \int_{\Omega^m} \delta u_{(i,j)}^m C_{ijkl}^m u_{(k,l)}^m d\Omega - \int_{\Gamma_n^m} h_i^m \delta u_i^m d\Gamma \right)$$

$$- (1-\beta)(1-\mu)\left\{ \int_{\Gamma_{int}} \langle \delta\sigma_{ij} \rangle_\gamma n_j^1 [\![u_i]\!] d\Gamma + \int_{\Gamma_{int}} [\![\delta u_i]\!] \langle \sigma_{ij} \rangle_\gamma n_j^1 \, d\Gamma \right\}$$

$$+(1-\beta) \int_{\Gamma_{int}} \alpha [\![\delta u_i]\!] [\![u_i]\!] d\Gamma - \beta \left\{ \int_{\Gamma_{int}} [\![\delta u_i]\!] f([\![u_i]\!])\, d\Gamma \right\} = 0$$

Therefore, the factor β controls the switch from the embedded finite element methods to the interface approach for modeling cohesive fracture where $\beta = 0$ represents the pre – failure stage and $\beta = 1$ represents the post – failure stage once a failure initial condition $T_n \geq T_n^{max}$ is satisfied. The factor $\mu = 0$ shows that Nitsche's method is used to weakly enforce displacement continuity at the uncracked interface in the pre – failure stage while $\mu = 1$ represents the penalty method.

2.5 Spatial discretization approach

The whole problem domain Ω is discretized by a set of elemental domains Ω_e as the background mesh. The interface Γ_{int} is then embedded in the underlying background mesh, which allows the discretization of an interface by defining a set of intersection points (Figure 4). To identify the position of the interface within the background mesh, a level set method is adopted (Osher and Fedkiw, 2002). The elements with all positive level-set values belong to subdomain Ω^1 and those with all negative level-set values belong to subdomain Ω^2, which are considered as bulk elements. Those with both positive and negative level-set values are identified as cut elements with embedded discontinuities, which are further considered as a superposition of two partial elements by following the approach proposed by Hansbo and Hansbo (2002, 2004). In this discretization approach, one partial element contributes to the discretization in Ω^1 while the other one contributes to Ω^2. Thus, the whole domain can be discretized into two separated meshes with the only overlap at the interface (Figure 5). For the finite element approximation of the solution field, it is

correspondingly considered as the decomposition of discretized sub solution fields. The solution field and variation can be written as:

$$u^h = \sum_{\Omega^m} \left(\sum_{i \in I^m} H^m N_i \, u_i \right)$$

$$\delta u^h = \sum_{\Omega^m} \left(\sum_{i \in I^m} H^m N_i \, \delta u_i \right)$$

Where m = 1, 2, I^m represents the set of nodes belonging to Ω^m in Figure 5, the characteristic function H^m is given by

$$H^m(x) = \begin{cases} 1 & if \; x \in \Omega^m \\ 0 & otherwise \end{cases}$$

To be specific, the overlapping cut element formulation for a triangular element is described in Figure 6.

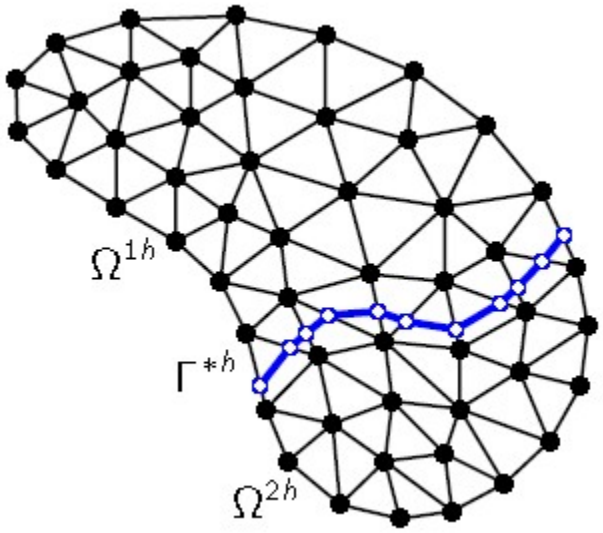

Figure 4: Representation of embedded interfaces

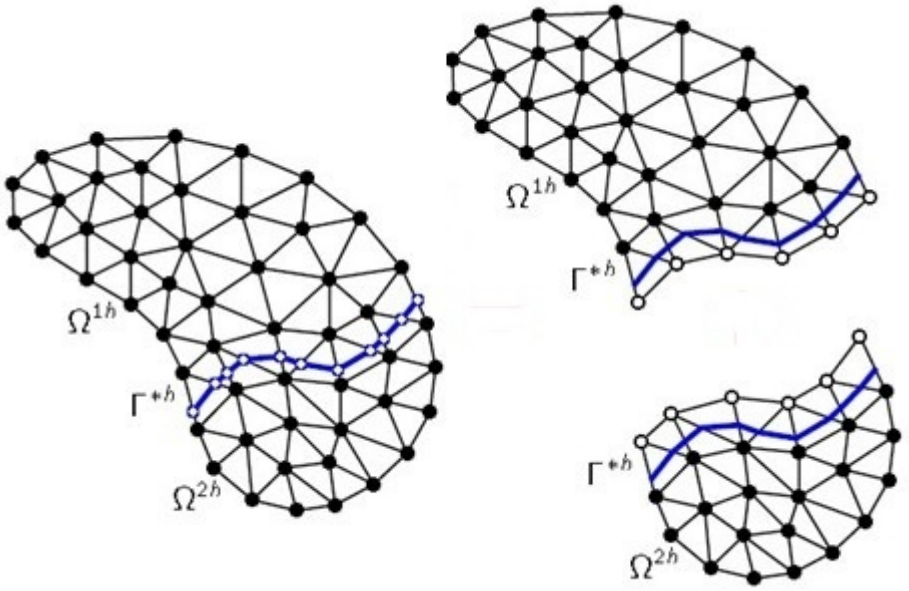

Figure 5: Discretized subdomains with overlap at the interface

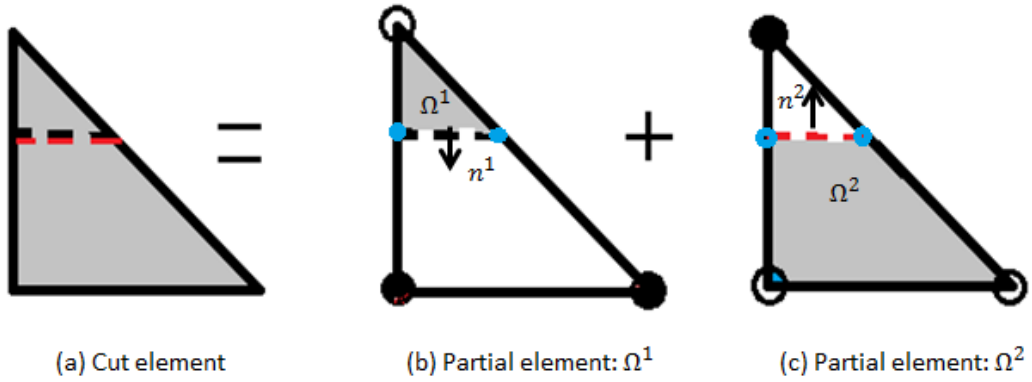

Figure 6: Overlapping element formulation for a triangular element cut by an embedded interface. Black circles are the physical nodes generalized in the background mesh and the hollow circles are the sibling nodes. The blue nodes represent the discretization of the embedded interface in each partial element.

2.5.1 Discrete formulation based on embedded finite element methods

By introducing the spatial discretization approach mentioned above into the weak formulation of the hybrid method, a system of semi discrete equations is given by

$$M\ddot{u} + Ku = F^{ext}$$

$$u(0) = u_0$$

$$\dot{u}(0) = \dot{u}_0$$

where $\ddot{u}, \dot{u}$ and u represent the nodal values of accelerations, velocities and displacements and the mass matrix M is given as

$$M = \begin{bmatrix} M_b^1 & 0 \\ 0 & M_b^2 \end{bmatrix}$$

The consistent mass matrix can be calculated as

$$M_b^m = \sum_e \int_{\Omega_e^m} N^T \rho^m N d\Omega_e \quad for\ m = 1, 2$$

However, a lumped mass matrix is often used in explicit dynamic schemes to prevent the inversion of the mass matrix at every time step and the stability of the time stepping schemes greatly depends on the mass lumping techniques particularly for embedded finite element methods. The details of mass lumping techniques are discussed later.

The stiffness matrix K in the pre – failure stage is given as

$$K = \begin{bmatrix} K_b^1 + K_n^1 + K_s^1 & K_c \\ K_c^T & K_b^2 + K_n^2 + K_s^2 \end{bmatrix}$$

where bulk stiffness terms in each subdomain are calculated as

$$K_b^m = \sum_e \int_{\Omega_e^m} B^T D^m B d\Omega_e \quad for\ m = 1, 2$$

Due to the presence of interfacial terms, the Nitsche and stabilization contributions are introduced into the leading diagonal and off-diagonal blocks of the stiffness matrix.

The Nitsche's contribution to the leading diagonal block is given by

$$K_n^m = -\gamma^m \sum_e \int_{\Gamma_{int}^e} N^T ((n^m)^T D^m) B d\Gamma_e - \gamma^m \sum_e \int_{\Gamma_{int}^e} B^T ((D^m)^T n^m) N d\Gamma_e \quad for\ m = 1, 2$$

while the stabilization term's contribution to the leading diagonal block is given by

$$K_s^m = \sum_e \alpha_e \int_{\Gamma_{int}^e} N^T N d\Gamma_e \quad for\ m = 1, 2$$

Also, their contributions to the off-diagonal block of the stiffness matrix K_c are calculated as

$$K_c = -\gamma^1 \sum_e \int_{\Gamma_{int}^e} N^T ((n^1)^T D^1) B d\Gamma_e - \gamma^2 \sum_e \int_{\Gamma_{int}^e} B^T ((D^2)^T n^2) N d\Gamma_e$$

$$- \sum_e \alpha_e \int_{\Gamma_{int}^e} N^T N d\Gamma_e$$

It is the stabilization term that accounts for the spatial stability of the above Nitsche's method, which restores the discrete system's positive definiteness influenced by the consistency and symmetry terms within the variational form. However, a lower value of α_e would upset the stability of the method while a higher value would offset

the advantages provided by variational consistency and hence make it behave similarly to the penalty method. Therefore, a careful choice of the stabilization parameter α_e is necessary in Nitsche's method to achieve stabilization.

Since the performance of Nitsche's method is effected by the stabilization parameter α_e, the value of α_e cannot be chosen in an arbitrary way as in the penalty method. Dolbow and Harari (2009) in their work have proposed a formulation to determine a minimum appropriate value of α_e in an element level for Nitsche's method and Annavarapu et al. (2012) has further extended this spirit to dynamic problems with remarkable revisions, which is discussed in the next section.

Remark: The discretized system of the penalty method can also be obtained from the above formulation by eliminating the Nitsche's contribution to the leading diagonal and off-diagonal blocks from the stiffness matrix, which corresponds to the switch factor μ.

The stiffness matrix K in the post – critical stage is given by

$$K = \begin{bmatrix} K_b^1 + K_t^1 & K_c \\ K_c^T & K_b^2 + K_t^2 \end{bmatrix}$$

The contribution of cohesive terms within the variational framework to the leading diagonal blocks is described as

$$K_t^m = \sum_e \omega \int_{\Gamma_{int}^e} N^T N d\Gamma_e \quad for\ m = 1, 2$$

where ω represents the characteristic constant of a certain cohesive law. For concreteness, in Ortiz and Pandolfi's cohesive law, $\omega = \begin{bmatrix} T_n^{max}/\delta_n & 0 \\ 0 & T_n^{max}/\delta_n \end{bmatrix}$. Similarly, their contribution to the off-diagonal blocks of the stiffness matrix is given by

$$K_c = -\sum_e \omega \int_{\Gamma_{int}^e} N^T N d\Gamma_e$$

Moreover, cohesive terms at the interface also contribute to the external force as

$$F^{coh} = \sum_e \varphi \int_{\Gamma_{int}^e} N d\Gamma_e$$

where $\varphi = [T_n^{max}; 0]$.

2.5.2 Evaluation of the stabilization parameters

Dolbow and Harari (2009) proposed an estimate for α_e from the positive definition of the discrete energy in scalar elliptic problems, which is given by

$$\alpha_e = \frac{1}{2} meas(\Gamma_{int}^e) \left(\frac{|D^1|}{meas(\Omega_e^1)} + \frac{|D^2|}{meas(\Omega_e^2)} \right)$$

However, α_e blows up for elements where either meas(Ω_e^1) or meas(Ω_e^2) tends to zero, which will cause severe constraints on the critical time step in explicit dynamic schemes since the maximum eigenvalue is a function of the stabilization parameter α_e. Following the spirit in Dolbow and Harari (2009), Annavarapu et al. (2012) proposed a general formula with the flexibility of choosing weights γ^1 and γ^2 as

$$\alpha_e = 2 * meas(\Gamma_{int}^e) \left(\frac{|D^1|(\gamma^1)^2}{meas(\Omega_e^1)} + \frac{|D^2|(\gamma^2)^2}{meas(\Omega_e^2)} \right)$$

which returns Dolbow and Harari's estimate by choosing $\gamma^1 = \gamma^2 = 0.5$. To solve the stability issues mentioned above, Annavarapu et al. (2012) defined the weights as $\gamma^m = meas(\Omega_e^1)/meas(\Omega_e)$, so the estimate formula is revised as:

$$\alpha_e = 2 * \frac{meas(\Gamma_{int}^e)}{\left(meas(\Omega_e)\right)^2}(|D^1|meas(\Omega_e^1) + |D^2|meas(\Omega_e^2))$$

This revised formulation of the stabilization parameter now only inversely varies with element size and provides a local fixed estimation for robustness. Here, no contrast of material properties is taken into consideration.

2.6 Temporal discretization

To date, it is important to note that no discretization with respect to time has been made. This semi-discrete approximation approach with time left continuous is specified as

$$u^h(x,t) = \sum_{\Omega^m}\left(\sum_{i\in I^m} H^m N_i(x)\, u_i(t)\right)$$

$$\delta u^h(x) = \sum_{\Omega^m}\left(\sum_{i\in I^m} H^m N_i\,(x)\delta u_i\right)$$

and only the nodal value $u_i(t)$ varies with time. The shape functions $N_i(x)$ are solely expressed in terms of the spatial discretization. Substituting the above expressions into the hybrid variational formulation and considering the arbitrariness of the weight functions yields the semi discrete system of equations

$$M\ddot{u}(t) + Ku(t) = F^{ext}$$

$$u(0) = u_0$$

$$\dot{u}(0) = \dot{u}_0$$

where $u(0)$ and $\dot{u}(0)$ are usually taken as initial nodal data.

2.6.1 Integration schemes

In the present work, the explicit central difference time–integration algorithms within the Newmark family are implemented in a residual form. The updating scheme for nodal displacement, accelerations and velocities from the n^{th} time step to the $(n+1)^{th}$ time step is given by

$$M\ddot{u} = R_{n+1} = F^{ext} - F^{int}_{n+1} + F^{coh}_{n+1}$$

$$u_{n+1} = u_n + \Delta t\, \dot{u}_n + \frac{1}{2}(\Delta t)^2 \ddot{u}_n$$

$$\ddot{u}_{n+1} = M^{-1} R_{n+1}$$

$$\dot{u}_{n+1} = \dot{u}_n + \frac{\Delta t}{2}(\ddot{u}_n + \ddot{u}_{n+1})$$

where Δt denotes the critical time step and R_{n+1} is the global residual vector which is assembled from all existing bulk elements and cut elements in each time step. It is a conditionally stable method with an above bound on the critical time step. The conditional stability is satisfied for

$$\Delta t \leq \frac{2}{\omega_{max}}$$

Here, ω_{max} is the maximum eigenvalue given by the generalized eigenvalue problem

$$(K - \omega^2 M)u = 0$$

It is obvious to see that the additional contributions to the stiffness matrix due to the penalty and consistency terms in the variational form have a significant influence on

the critical time step for temporal stability in addition to the mass lumping techniques adopted in the updating schemes.

2.6.2 Stability analysis

Instead of estimating the critical time step from the global stiffness matrix and mass matrix, a more robust approach is proposed to evaluate Δt at an element level:

$$(k_e - \omega_e^2 m_e)u_e = 0 \qquad \Delta t_e \leq \frac{2}{\omega_e^{max}}$$

In this way, the systemic critical time step Δt is defined as the minimum value in the set of $\{\Delta t_e\}$, which is proved to be a smaller estimate than the one obtained from a global evaluation (Hughes, 1979).

Particularly with embedded constrained interfaces, the critical time step Δt_e of cut elements naturally depends on the location of the interface $\varepsilon \in [0,1]$ and the parameter α_e. A 1D case is shown in Figure 7. It is direct to lump the mass of both partial elements with their physical mass by following the spirit in Menouillard's work (2008), so that

$$m_e = \begin{bmatrix} \varepsilon m_e^{classic} & 0 \\ 0 & (1-\varepsilon) m_e^{classic} \end{bmatrix}$$

Then, by enforcing the continuity constraints at the interface through the penalty method, I obtain the stiffness matrix such that

$$k_e = \begin{bmatrix} \varepsilon k_e^{classic} + k_e^{pen} & -k_e^{pen} \\ k_e^{pen} & (1-\varepsilon) k_e^{classic} + k_e^{pen} \end{bmatrix}$$

$$k_e^{pen} = \alpha \begin{bmatrix} (1-\varepsilon)^2 & (1-\varepsilon)\varepsilon \\ \varepsilon(1-\varepsilon) & \varepsilon^2 \end{bmatrix}$$

The maximum eigenvalue can be calculated as $\omega_e(\alpha, \varepsilon) = \text{eigs}\{k_e(\alpha, \varepsilon), m_e\}$. Annavarapu et al. (2012) stated that as the distance of an interface $\varepsilon h_e \to 0$ or $\varepsilon h_e \to 1$, the maximum eigenvalue $\omega_e^{max} \to \infty$ and hence $\Delta t_e \to 0$ with the choice of parameter as $\alpha = E/h_e$. Thus, he concluded that the above direct mass lumping techniques for only discontinuous elements cannot be extended to complex dynamic problems when constraints are enforced at the interface.

He also proposed a new mass lumping technique developed for extended finite element methods with constraints at the interface. To prevent the dependence of ε in the overlapping elemental mass matrix, the total element mass is equally distributed on all elemental nodes as diagonal entries of the mass matrix, regardless of the position of the embedded discontinuities. Now the new lumped mass matrix independent of ε is given by

$$m_e = \frac{m_{total}}{4}\begin{bmatrix} 1 & 0 & 0 & 0 \\ 0 & 1 & 0 & 0 \\ 0 & 0 & 1 & 0 \\ 0 & 0 & 0 & 1 \end{bmatrix}$$

which prevents issues associated with infinite nodal masses. It contributes that $\omega_e(\alpha, \varepsilon) = \text{eigs}\{k_e(\alpha, \varepsilon), m_e\}$ and the maximum eigenvalue $\omega_e^{max}(\varepsilon) \to 0$ when introducing $\alpha = \text{E}/h_e$ as the distance of an interface $\varepsilon h_e \to 0$ or 1. It can be easily extended into multi-dimensional cases.

Therefore, issues associated with a null critical time step are prevented by the Annavarapu et al. (2012) lumping techniques which hence contribute to the temporal stability of extended finite element methods with interfacial constraints to simulate

dynamic crack propagation problems. In addition, by using the new mass lumping techniques, the maximum eigenvalue can be solved again from the generalized equation $\det(m_e^{-1}k_e - \omega^2 \mathrm{I}) = 0$ when introducing $\varepsilon = 0.5$, so that

$$\omega_{max}^2(\alpha) = \left\{0 \ \frac{4\alpha}{h_e\rho} \ \frac{4E}{h_e^2\rho} \ \frac{4E}{h_e^2\rho}\right\}$$

$\omega_{max}^2 \propto \alpha$, which implies that the larger penalty parameters α lead to smaller critical time steps. It is easy to see that the choice of parameter α not only affects the spatial stability and convergence rates, but also affects the temporal stability of time-integration schemes.

Recall the penalty method and Nitsche's method described in the spatial discretization. Within Nitsche's methods, penalty terms are only necessary for the spatial stabilization and the stabilization parameter is evaluated and bounded from the positive definiteness of the discrete system. Otherwise, if the positive definiteness is denied, the discrete energy growing in time leads to unstable time-integration schemes. Obviously, when using the standard Nitsche's method with $\gamma^1 = \gamma^2 = 0.5$, the stabilization parameter α_e inversely varies with ε and $(1 - \varepsilon)$ in the 1D case shown in Figure 7. When $\varepsilon \to 0$ or 1, the stabilization parameter $\alpha_e \to \infty$ and hence Δt_e tends to zero. As a result, the critical time step is severely restricted and the computational cost of explicit dynamic schemes increases. To prevent the above issues associated with $\varepsilon \to 0$ or 1, the weighted Nitsche's method with $\gamma^m \in (0,1)$ is suggested to make α_e remain bounded regardless of the position of the interface. That means, weighted Nitsche's method is recommended for the temporal stability when the interface is not located in

the middle of an element. Therefore, the generally robust explicit dynamic schemes for crack propagation are implemented with the Annavarapu et al. (2012) mass lumping techniques and weighted Nitsche's method in the following numerical examples.

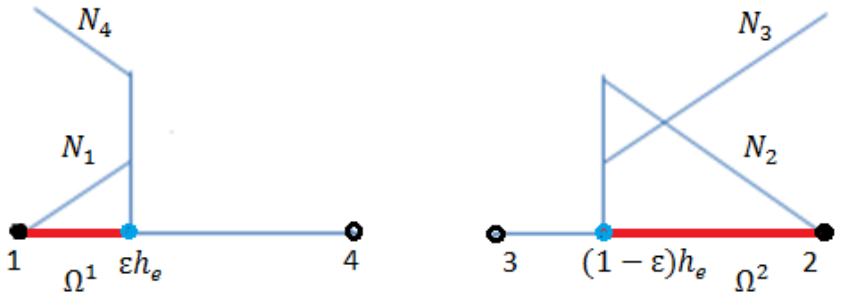

Figure 7: Illustration in 1D case for the interface position: the black nodes are physical nodes of background mesh and hollow nodes are siblings. The blue ones represent the embedded interface. The position of the interface is defined by a distance from the interface node to the physical node.

3. Numerical examples

In this chapter, wave propagation tests and dynamic crack propagation examples are provided to illustrate the application of the new hybrid numerical schemes proposed in Chapter 2.

In the first wave propagation test problem, I investigate and compare the performance of embedded constraint methods for modeling the pre-failure stage in dynamic processes. For the penalty method and Nitsche's method, I use the explicit central difference time-integration scheme with Annavarapu et al. (2012) mass lumping techniques. When implementing the standard form of Nitsche's method within explicit methods, the parameters used are $\beta = 0$ and $\gamma^m = 0.5$ for second-order accuracy. The weighted Nitsche's method is denoted as γ Nitsche throughout this chapter with γ^m calculated respectively. These methods are chosen and controlled by setting up switch factors in numerical schemes.

For the second example of simulating dynamic crack initiation and propagation under sine loading, I implement an extrinsic linear cohesive law on embedded interfaces for modeling the extrinsic CZM in the post-critical stage. The performance of embedded constraint methods in tension and compression cases are also investigated here, since these methods have a significant influence on accurately initializing and implementing cohesive laws when a fracture criterion is met.

3.1 Wave propagation tests

In Chapter 2, it has been seen that the emerging of embedded discontinuities within finite element methods can affect the robustness of the explicit time integration scheme. To further investigate the performance of embedded methods in the pre-failure stage of dynamic processes, specific wave propagation tests are discussed below.

Consider a square block with length $L = 1mm$ and height $H = 1mm$ as shown in Figure 8. This specimen consists of two parts with the same elastic material properties that are separated by an embedded planar interface located at 0.4876mm from the bottom edge. The top edge of the specimen is subjected to a sine loading that is prescribed as $f^{ext} = \sin(20\pi t)$, while the bottom edge is traction-free. The material in this case is characterized by a Young's modulus $E = 10^3 N/m^2$, the Poisson's ratio $\gamma = 0$ and mass density $\rho = 10kg/m^3$.

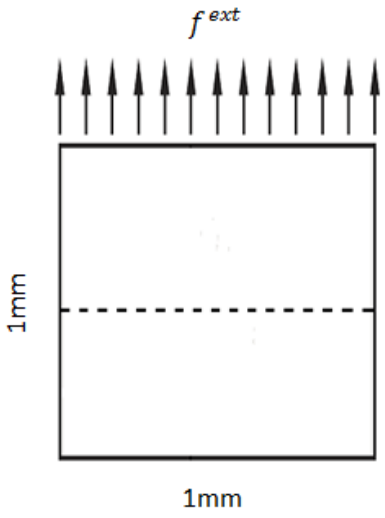

Figure 8: Geometry model and loading conditions in wave propagation tests

The embedded simulations are carried out on a structured constant strain triangle mesh with 10 divisions along each direction for the total simulation time T = 0.1s. By setting the cohesive strength as a pretty large value that can be impossibly reached, the simulations can be only constricted in the pre – failure stage of the whole dynamic process.

First of all, I investigate the performance of the penalty method in the pre-failure stage. An interface is embedded in the pre-failure region with the help of penalty method to weakly enforce the perfect continuity. Usually, the penalty parameter scales inversely with the mesh size h_e and is of the k^{th}order of magnitude as E, where the relationship between penalty parameter α and E is simply denoted as $\alpha = 10^k E$. It is obvious that the penalty parameter is of the same order of magnitude as E when k = 0, so that the penalty terms grow at the same rate as the other classical stiffness terms. However, in order to obtain accurate solutions with the penalty method, a larger value of the penalty parameter is necessary, although it might directly result in ill-conditioning issues and adversely affect critical time steps. Large parameters also cause unphysical oscillations in the interfacial tractions, which will be questionable to further initialize cracks and implement cohesive laws.

The tractions of all interfacial gauss points before a crack is initialized are plotted in Figure 9, which varies with different penalty parameters yet at the same actual time $t = 0.026s$.

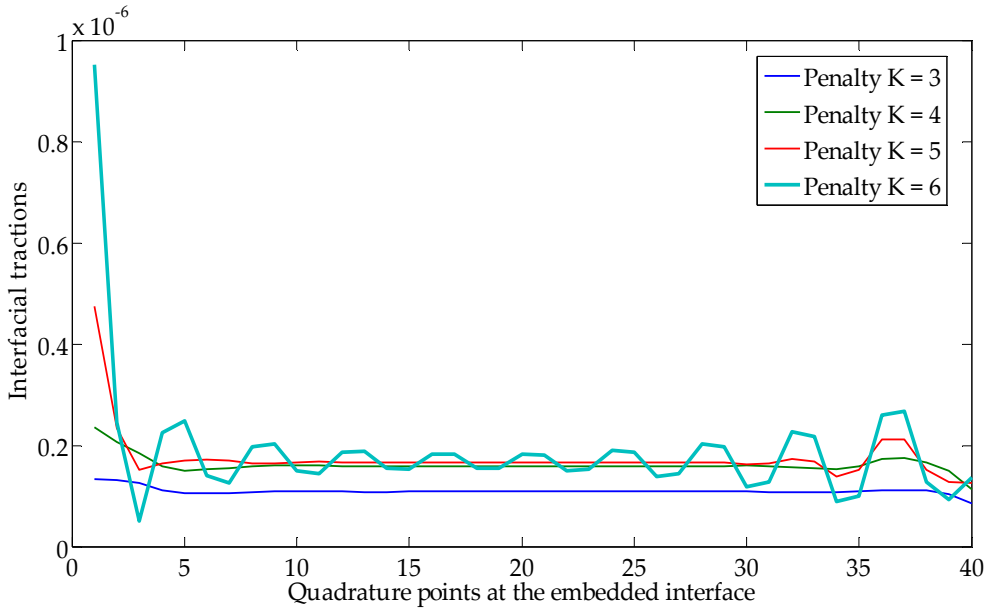

Figure 9: Interfacial tractions at the embedded interface with variation of different penalty parameters where k = log10 (α /E)

Figure 9 shows that the interfacial tractions tend to accurate values as the penalty parameter increases. However, the interfacial tractions become unstable when k is greater than 4. The unphysical oscillations of the interfacial tractions would make the fracture initial condition of a certain gauss point inaccurately satisfied and hence introduce perturbations into the crack propagation.

To investigate the effect of h_e on the performance of the penalty method, I refine the background mesh with 40 divisions along the x direction. A similar plot is shown in Figure 10. Traction oscillations in greater magnitude can be seen along the embedded

interface, especially on two sides.

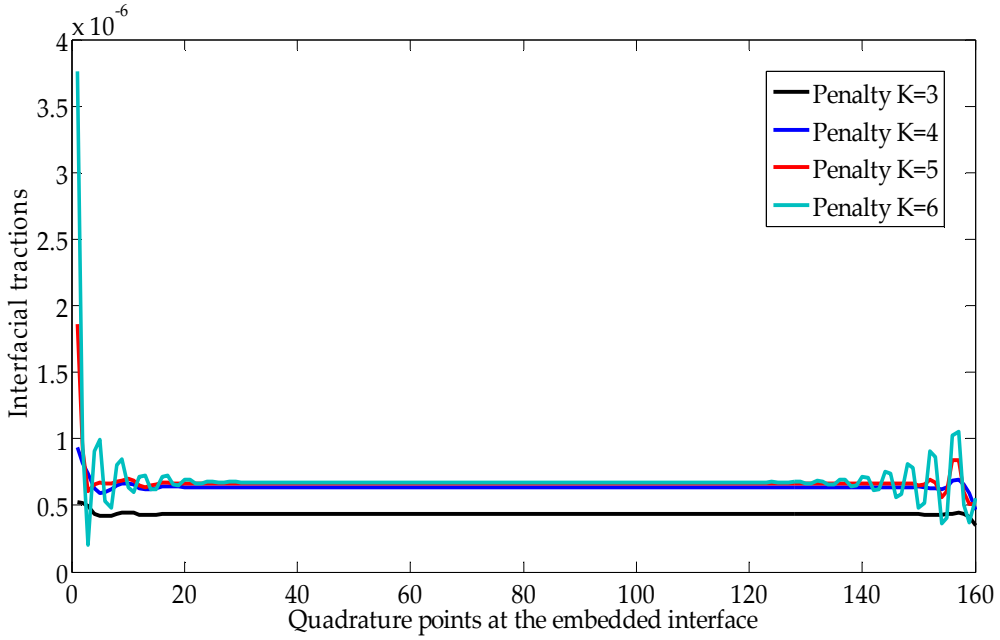

Figure 10: Interfacial tractions at the embedded interface with variation of different penalty parameters where k = log10 (α /E)

Furthermore, the effects of the penalty method, standard Nitsche's method and weighted Nitsche's method on the interfacial tractions at the actual time t = 0.06s are compared in Figure 11 for the case where the interface is not embedded at the middle of an element. When the interface is located at $y = 0.4876mm$, it is interesting to note that even the standard Nitsche's method leads to minor traction oscillations at the interface while the large penalty parameter cannot guarantee stable interfacial tractions.

On the other hand, it is also significant to figure out the upper bound of penalty parameters for a reasonable critical time step. Although the effect of large penalty parameters on the temporal stability is well-known, the specific curve of critical time steps varying with increasing penalty parameters remains unknown. In Figure 12, I

normalize the critical time step with that of a standard finite element and plot it against k. Clearly, the critical time step decreases quickly when k is greater than 5 and tends to zero with increasing penalty parameters.

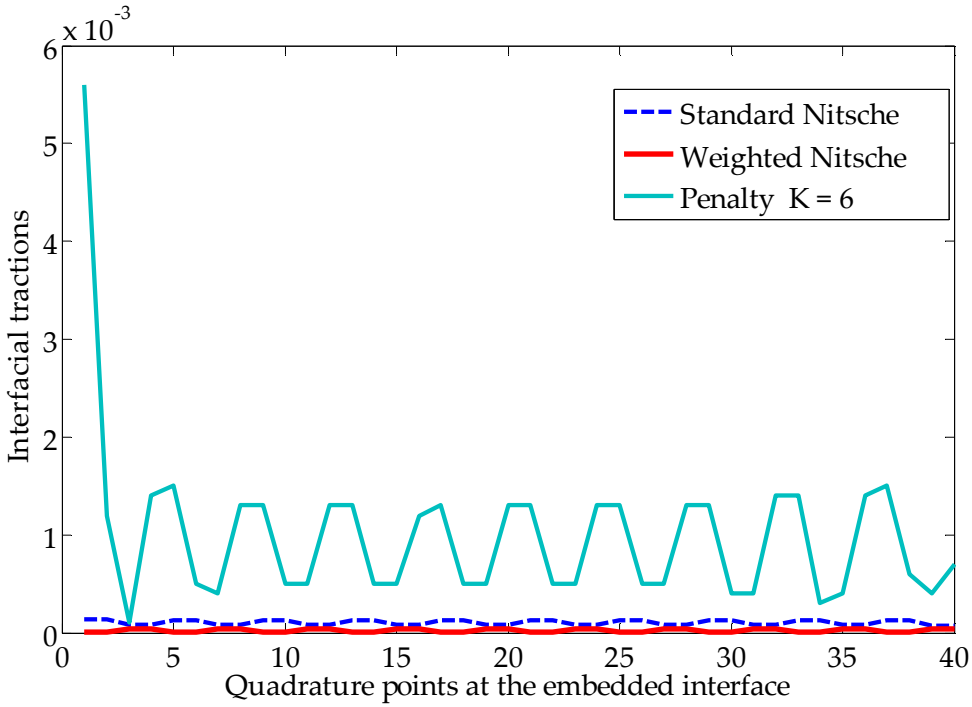

Figure 11: Comparison of interfacial tractions at the embedded interface with different embedded methods

Therefore, the penalty parameter within the penalty method has an upper bound such that k is not greater than 4 to retain both temporal stability and stable interfacial tractions. By adding the consistency terms, Nitsche's method guarantees the stability of tractions at the interface with local stabilization parameters evaluated at an element level for modeling the pre-failure stage of dynamic fracture, especially the weighted Nitsche's method that is suggested when the interface is not embedded at the middle of an element.

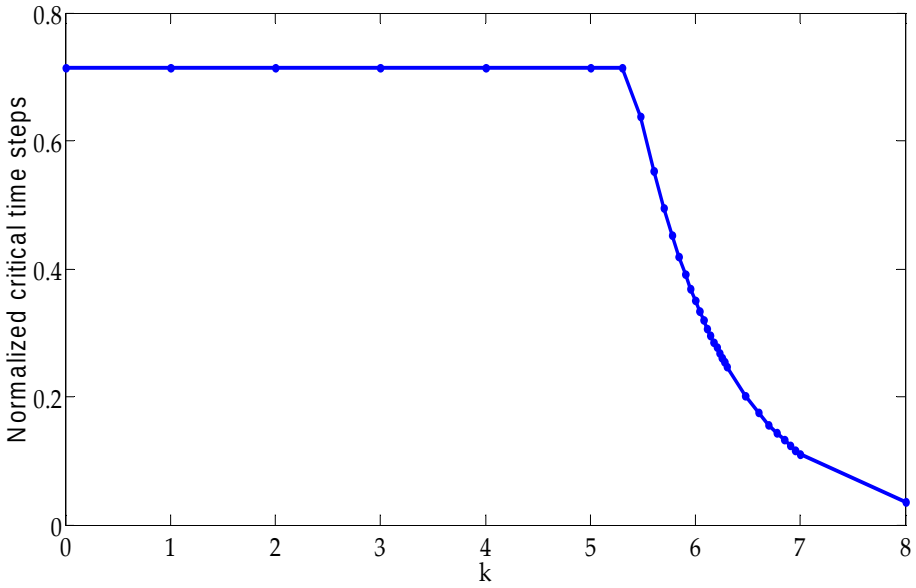

Figure 12: Variation of critical time steps with increasing penalty parameters

3.2 Dynamic crack propagation

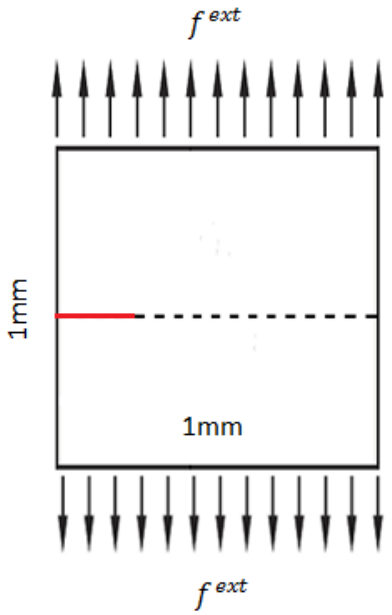

Figure 13: Geometry model and loading conditions in dynamic crack propagation

In this section, the hybrid numerical schemes combining the embedded finite element method and interface approach are used to simulate crack initiation and propagation. The performance of the penalty method and Nitsche's method for initializing cracks in the post- failure stage of dynamic fracture are investigated. Comparisons are made in the following tension and compression cases respectively.

The geometry and loading conditions of the model problem are illustrated in Figure 13. Consider a $1mm$ by $1mm$ square block, which is made of the material with a Young's modulus $E = 3.24GPa$, Poisson's ratio $\gamma = 0$ and density $\rho = 1190kg/m^3$ and contains an initial crack that penetrates $a = 0.25mm$ into the material. The block is loaded by sine loadings that are applied to the top and bottom edges respectively. Because of the symmetry, it is assumed that the crack will propagate along the embedded interface as a straight line after the initiation condition is satisfied. The initial crack is modeled as traction free. When the initial crack propagates, Ortiz and Pandolfi's CZM (1999) is used to characterize cohesive fracture processes. This model assumes that the opening interface carries forces that oppose separation between two surfaces until fully failed. The magnitude of the forces is a function of the relative separation.

In the following cases, only normal components of cohesive traction and separation are taken into consideration. For this linear extrinsic initially rigid cohesive model in Figure 3, the normal cohesive strength of the material is set to $T_n^{max} = 100MPa$ and the fracture toughness is prescribed as $G_{Ic} = 700N/m$. The characteristic length of the cohesive law is determined by the critical normal opening displacement $l_{n,cr}$ where

the crack has fully developed and the tractions have reduced to zero. This parameter is related to the fracture toughness G_{Ic} or the area under the softening curve and can be determined as follows:

$$l_{n,cr} = 2\ G_{Ic}/T_n^{max}$$

The fracture initiation condition is described as $T_n \geq T_n^{max}$.The behavior of the opening surfaces in tension are governed by the traction-separation relationship described in Section 2.3.1. Once the maximum normal cohesive traction is reached, the weakly embedded interfaces starts opening and the traction linearly reduces to zero up to the maximum separation $l_{n,cr}$. After that, the cut elements with embedded discontinuities are considered to be failed and a crack is initialized along the interface.

The block is analyzed on a structured constant strain triangle mesh with 40 divisions along each direction, so that the element length is $h_e = 12.5\mu m$ which is smaller than $l_{n,cr}$. Remmers (2008) investigated that adding new degrees of freedom during a simulation does not affect the energy conservation such that the sum of internal and kinetic energies in the system is up to the total external work regardless of the mesh. His studies also suggested that only the simulation carried on a dense mesh with $h_e \leq l_{n,cr}$ guaranteed the accuracy of total energy. Thus, a dense mesh with $h_e = 12.5\mu m$ is satisfied with this condition and used in the following simulations.

3.2.1 Implemental aspects of the extrinsic CZM

For the numerical implementation, the embedded flux terms for enforcing perfect continuity give place to the extrinsic cohesive law governing the fracture

processes in the material after the fracture criterion is met. The normal tractions at the interface are considered as interfacial constrains, so the additional cohesive terms are introduced into the weak form as interfacial integrals which contribute to the stiffness matrix and nodal forces. By using a transformation matrix, the computed forces are then transformed into the global coordinates. It should be noticed that such numerical schemes do not require any modifications of the mesh, yet simply a change in the terms. The interfacial integrals are carried out using a two point Gauss Quadrature rule at the interface, which leads to another significant advantage that the cohesive law operates strictly at each quadrature point. It implies that both cracked and uncracked quadrature points are allowed within a cut element at the same time. This advantage affords the possibility of sub-element cracks. In the extrinsic CZM, all quadrature points of cut elements simultaneously respond according to the traction and separation relationship when the fracture criterion is met at a single point. In each time step, the evaluation of the fracture criterion is done for all quadrature points in order to assemble their contributions to the global residual vector.

Furthermore, the evaluation of the fracture criterion at each quadrature point is effected by the embedded methods in the pre-failure stage. As previously mentioned, the initial slope of this extrinsic cohesive law should ideally be infinite as well as the stiffness of initial interfaces. The separation is only initialized when the current interfacial traction T_n reaches the cohesive strength T_n^{max}. However, within the penalty method, an unphysical dummy initial slope usually appears when calculating the

interfacial traction and the jump in displacement for the evaluation of the fracture criterion. The magnitude of the initial slope is exactly the penalty parameter α. In other words, the penalty parameters have a significant influence on the crack initiation and how to prevent the dummy slope requires further investigations. By contrast, the performance of Nitsche's method in dynamic crack initiation and propagation are investigated.

To be particularly mentioned during unloading, when the normal separation $[\![u]\!]_n$ becomes negative in compression, this interpenetration of interfaces should be prevented. Usually, self-contact is simulated by using a penalty stiffness parameter that tends to infinity, and the compressive traction at the interface is calculated by $T_n = \alpha[\![u]\!]_n$. Its performance in compression is not reliable. By contrast, Nitsche's method is recently highlighted to prevent the interpenetration under unloading by weakly enforcing the contact condition $[\![u]\!]_n = 0$.

3.2.2 Crack propagation only in tension

In this section, to illustrate the effect of the penalty parameter on crack initiation, I capture the interfacial tractions and separations at a certain interfacial gauss point through all time steps. Figure 14 shows several normalized traction – separation laws implemented with different penalty parameters at the same interfacial gauss point. From the plot, we can see that the unphysical initial slope becomes sharper with increasing penalty parameter. It is also obvious that a large penalty parameter is necessary in order to minimize the dummy slope.

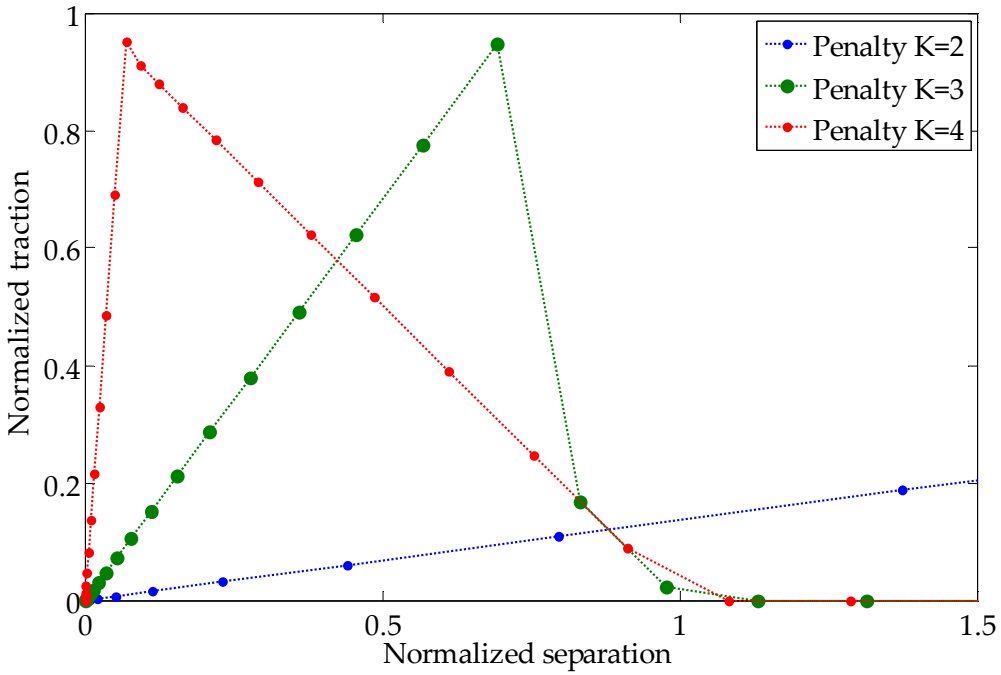

Figure 14: Implemented an extrinsic linear cohesive law based on different penalty parameters

Considering the stabilization of explicit dynamic schemes and stable interfacial tractions, penalty parameters are limited such that k is no more than 4. Although it seems reasonable to increase the penalty parameter in order to prevent the dummy initial slope and gain the accurate implementation of the extrinsic cohesive law, issues in dynamic schemes are triggered when k is greater than 4. Moreover, it is difficult to know in advance how large the penalty parameter should be for the accurate implementation.

From Figure 15, we can see that the dummy initial slope is eliminated by Nitsche's method where the stabilization parameters are locally evaluated at an element level and have no effects on the initial slope. In other words, Nitsche's method is much

more robust than penalty method for the implementation of extrinsic cohesive laws, since it keeps us from choosing large parameters in an arbitrary sense.

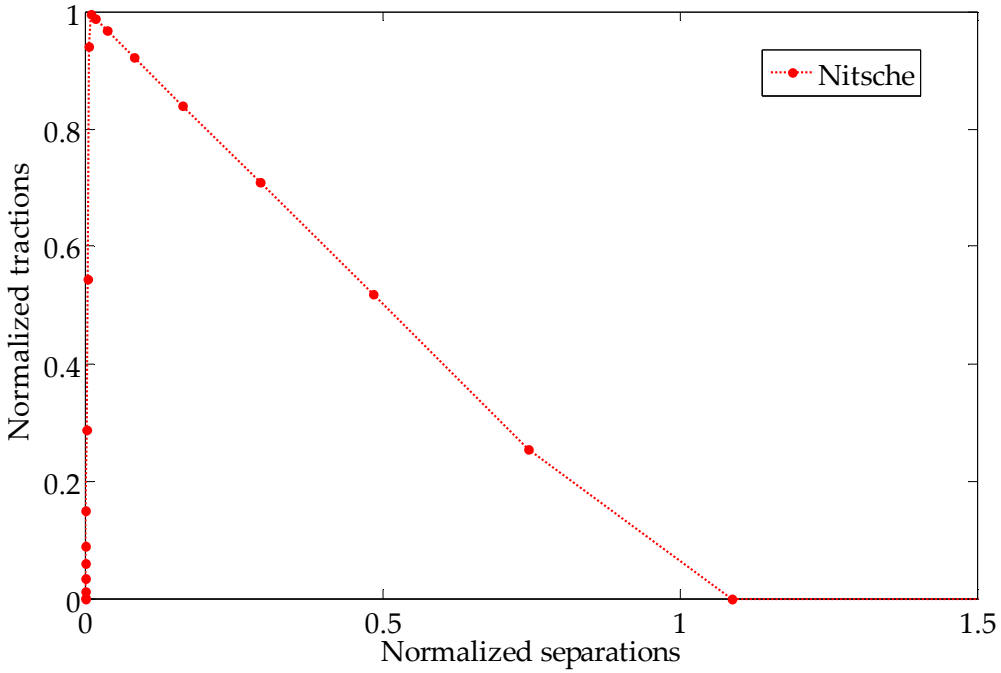

Figure 15: Implemented an extrinsic cohesive law with Nitsche's method

Then, I compare the curves based on penalty method to that of Nitsche's method through choosing different penalty parameters. From the plot in Figure 16, the penalty method performs similarly as Nitsche's method when the k is roughly around 5 or greater. Thus, taken the upper bound k = 4 into consideration, it implies that the penalty method can't guarantee the accurate implementation of extrinsic cohesive laws without negatively impacting the stable time step.

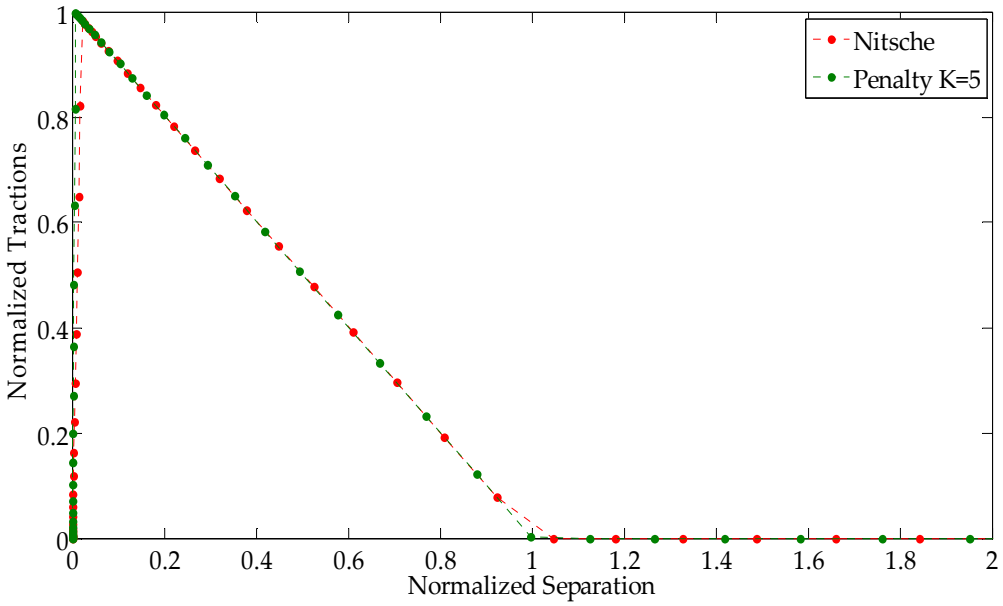

Figure 16: Comparison of Penalty method and Nitsche's method in implementation of an extrinsic cohesive law

3.2.3 Crack propagation in both tension and compression

To simulate the whole dynamic fracture processes under loading and unloading, the case including both tension and compression should be taken into consideration in this section. The same problem in Figure 13 is simulated both with penalty method and Nitsche's method combining with an extrinsic CZM for the purpose of comparison. Although the specific parameters of the materials and the responding extrinsic cohesive law are not really important when numerically investigating the performance of these embedded methods, the same materials properties are used for consistency. The solution is computed from two types of methods using the same structured dense mesh in the last section.

Figure 17 shows the variation of tractions and separations at a certain quadrature point when the model is subjected to sine loadings on both edges. From the plot, we can see that Nitsche's method performs better than the penalty method in compression in term of preventing the interpenetration.

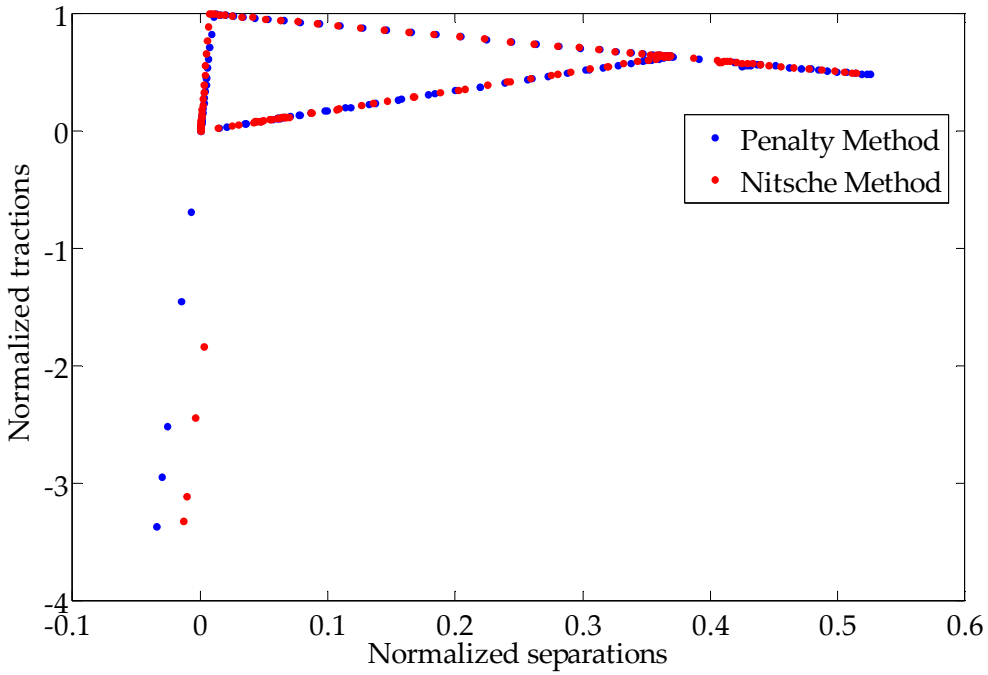

Figure 17: Comparison of Penalty method (k=5) and Nitsche's method in compression for preventing interpenetrations

By numerically enforcing $[\![u]\!]_n = 0$ at quadrature points in compression, Nitsche's method maintains the negative numerical results within an acceptable tolerance, which makes the slope of the compressive curve of the traction and separation relationship close to infinity. Since Nitsche's method has advantages of initializing cracks and preventing the interpenetration of closed crack surfaces, they afford the

possibility of accurately implementing extrinsic cohesive laws and hence are suggested in the simulation of dynamic crack propagation.

The corresponding stress contour and displacement field at different times based on Nitsche's method are displayed by ParaView in Figure 18. The total time is 5.0e-8s, which is also the period of the sine loading operating on both edges. We can see that the crack propagates when the fracture criterion is met and closes under compressive loading after t = 2.5e-8s.

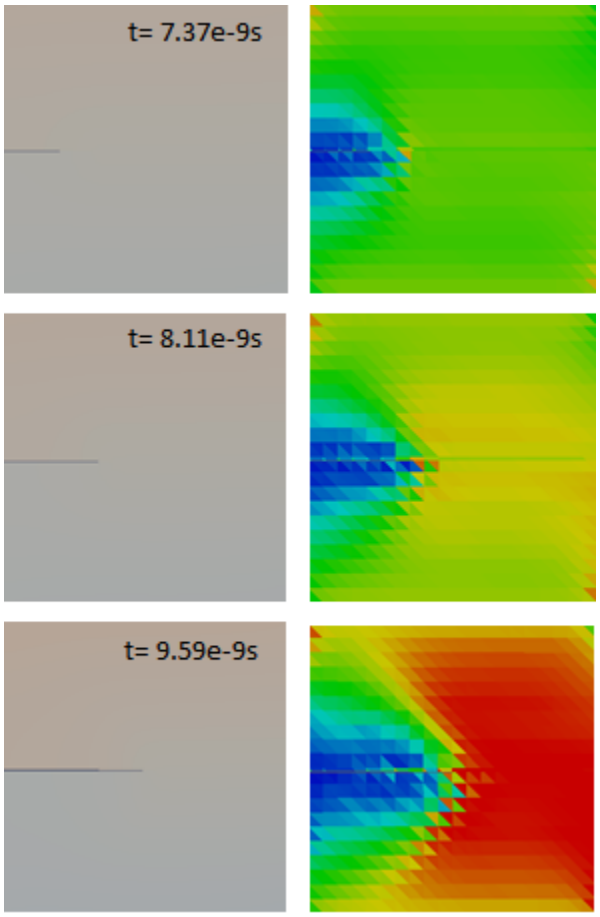

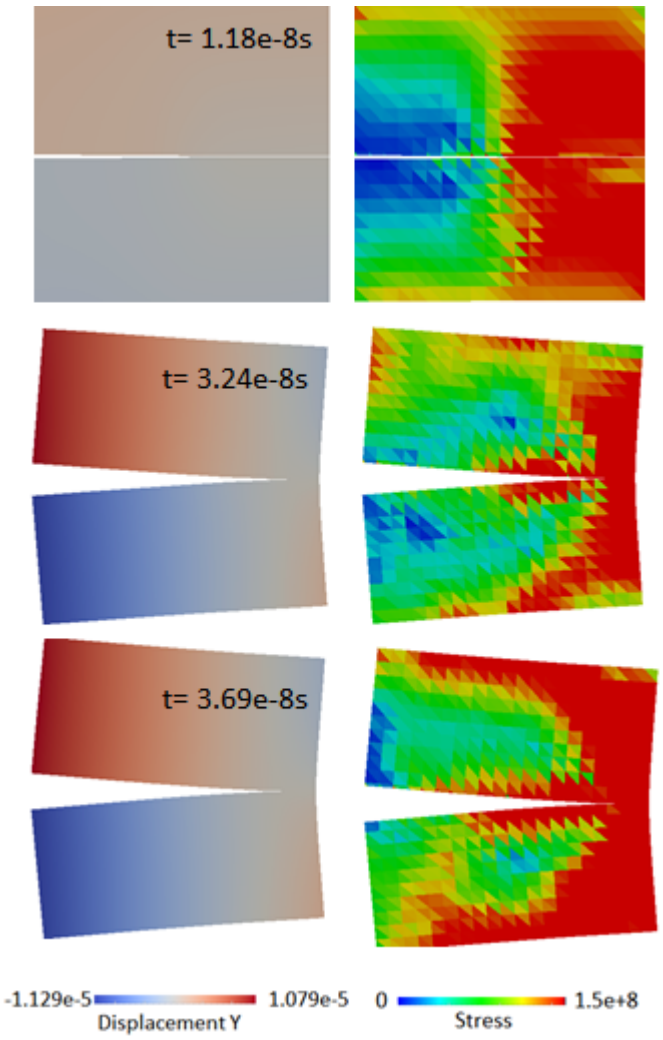

Figure 18: Stress and Displacement field at different times

4. Conclusions

In this thesis, a hybrid embedded finite element method/CZMs was presented for modeling dynamic crack initiation and propagation in brittle materials. This method is based on a combination of embedded finite element methods and extrinsic cohesive zone models. I investigated the effect of different methods to enforce kinematics at the embedded interface on the simulation of crack initiation and propagation.

The severe restrictions on the stable time step and stable interfacial tractions resulting from the arbitrary choice of penalty parameters were highlighted in explicit dynamic schemes. For improvements, additional terms for consistency and stabilization were introduced into the finite element framework by Nitsche's method in the pre-failure stage. The main advantage of the proposed hybrid scheme was shown that Nitsche's method guaranteed the temporal stability and stable tractions at the uncracked interface with the evaluation of local stabilization parameters at an element level, which provides more accurate evaluations of the fracture criterion.

Then, another advantage was also observed that Nitsche's method with local stabilization parameters prevented the unphysical initial slope in the numerical implementation of extrinsic cohesive laws, which affords us more accurate crack initiation than using penalty method. When the fracture criterion was met, the extrinsic cohesive law governed the behavior of the opening surfaces by a simple change of framework without modifications of the mesh, which avoids the issues on parallel simulations and topological structures necessary for inter-element methods. The

interface approach was used to directly implement the traction and separation law at the interfacial integration points that were naturally introduced within embedded algorithms.

Importantly, Nitsche's method provides better results than the penalty method conventionally used to prevent interpenetration in compression cases. Upon closure of the crack surfaces, the negative numerical results within an acceptable tolerance were computed with Nitsche's method by weakly enforcing contact conditions at the crack surfaces. Thus, this hybrid method is suggested in the simulation of dynamic crack initiation and propagation under loading and unloading. With the help of Nitsche's method, it has the advantages of initializing cracks and preventing the interpenetration of closed crack surfaces, which affords the possibility of accurately implementing extrinsic CZMs incorporated into finite element methods.

References

Annavarapu C, Hautefeuille M, Dolbow J. (2012), "Stable imposition of stiff constraints in explicit dynamics for embedded finite element methods". *Int. J. Numer. Meth. Engng.;* In revision.

Barenblatt, G.I., 1959. "The formation of equilibrium cracks during brittle fracture: General ideas and hypothesis, axially symmetric cracks". *Applied Mathematics and Mechanics (PMM)* 23, 622–636.

Barenblatt, G.I., 1962. "Mathematical theory of equilibrium cracks in brittle fracture". In: Dryden, H.L.,von Karman, T. (Eds.), *Advances in Applied Mechanics*, vol. 7, pp. 55–125.

Brian N. Cox, Huajian Gao, Dietmar Gross, Daniel Rittel, "Modern topics and challenges in dynamic fracture", *Journal of the Mechanics and Physics of Solids*, Volume 53, Issue 3, March 2005, Pages 565-596.

Belytschko, T., Chen, H., Xu, J. and Zi, G. (2003), "Dynamic crack propagation based on loss of hyperbolicity and a new discontinuous enrichment". Int. J. Numer. Meth. Engng., 58: 1873–1905.

Becker G., L. Noels, "A fracture framework for Euler-Bernoulli beams based on a full discontinuous Galerkin formulation/extrinsic cohesive law combination", *Int. J. Numer. Methods Engrg.*, 1097-0207, 85 (10) (2011), pp. 1227–1251.

Camacho GT, Ortiz M. "Computational modeling of impact damage in brittle materials". *International Journal of Solids and Structures* 1996; **33**:2899–2938.

Cockburn B, Karniadakis GE, Shu CW. "Discontinuous Galerkin Methods: Theory, Computation and Applications". Springer: Berlin, 2000.

Dooley I, Mangala S, Kale L, Geubelle P. "Parallel simulations of dynamic fracture using extrinsic cohesive Elements". *Journal of Scientific Computing* 2009; **39**(1):144–165.

Douglas J, Dupont T. "Interior penalty procedures for elliptic and parabolic Galerkin methods". *In Computing Methods in Applied Science, Lecture Notes in Physics*, vol. 58. Springer: Berlin, 1976; 207–276.

Fries T.P. and T. Belytschko. "The extended/generalized finite element method: An overview of the method and its applications". *Internat. J. Numer. Methods Engrg.*, 84:253 – 304, 2010.

Hansbo A, Hansbo P (2004) ,"A finite element method for the simulation of strong and weak discontinuities in solid mechanics". *Comput Meth Appl Mech Eng* 193:3523–3540.

Hansbo A, Hansbo P. "An unfitted finite element method, based on Nitsche's method, for elliptic interface problems". *Comput. Methods Appl. Meth. Engrg*. 2002; 191(47-48): 5537-5552.

Hughes TJR, Pister KS, Taylor RL. "Implicit - explicit finite elements in nonlinear transient analysis". *Computer Methods in Applied Mechanics and Engineering* 1979; 17-18(Part 1): 159 – 182.

Juntunen M, Stenberg R. "Nitsche's method for general boundary boundary conditions". *Math. Comp* 2009;78(267):1353-1374.

Klein P., J. Foulk, E. Chen, S. Wimmer, H. Gao, "Physics-based modeling of brittle fracture, cohesive formulations and the applications of meshfree methods", *Theoret. Appl. Fract. Mech*. 37 (2001) 99–166.

Mergheim J., E. Kuhl, P. "Steinmann, A hybrid discontinuous Galerkin/interface method for the computational modelling of failure", *Commun. Numer. Methods Engrg.* 20 (2004) 511–519.

Menouillard T, Rethore J, Moes N, et.al. "Mass lumping strategies for X-FEM explicit dynamics: Application to crack propogation". *Int. J. Number. Meth. Engng*. 2008; 74(3):447-474.

Moës N. , Dolbow J. , and T. Belytschko. "A finite element method for crack growth without remeshing". *Internat. J. Numer. Methods Engrg.*, 46:131 – 150, 1999.

Nitsche J. , Uber ein variations zur luosung von dirichlet-problemen bei verwendung von teilr€aumen die keinen randbedingungen unterworfen sind, *Abh. Math*. Se. Univ. 36 (1970) 9–15.

Ortiz M, Pandolfi A. "Finite-deformation irreversible cohesive elements for three-dimensional crack-propagation analysis". *International Journal for Numerical Methods in Engineering* 1999; **44**:1267–1282.

Osher S, Fedkiw R. "Level Set Methods and Dynamic Implicit Surfaces", vol. 153. Springer-Verlag, 2002.

Pandolfi A, Ortiz M. "An efficient adaptive procedure for three-dimensional fragmentation simulations". *Engineering with Computers* 2002; **18**:148–159.

Papoulia KD, Sam CH, Vavasis SA. "Time continuity in cohesive finite element modeling". *International Journal for Numerical Methods in Engineering* 2003; **58**:679–701.

Radovitzky R, Seagraves A, Tupek M, Noels L. "A hybrid dg/cohesive method for modeling dynamic fracture of brittle solids". *Computer Methods in Applied Mechanics and Engineering*, submitted.

Réthoré J, Gravouil A, Combescure A (2004) "A stable numerical scheme for the finite element simulation of dynamic crack propagation with remeshing". *Comput Meth Appl Mech Eng* 193:42–44.

Réthoré J, Gravouil A, Combescure A (2005) "An energyconserving scheme for dynamic crack growth using the extended finite element method". *Int J Numer Meth Eng* 63:631–659.

Remmers, J.J.C., de Borst, R., Needleman, A., "A cohesive segments method for the simulation
of crack growth", *Computational Mechanics*, **31**, 69.77, 2003.

Ravi-Chandar K, Yang B. "On the role of microcracks in the dynamic fracture of brittle materials". *Journal of the Mechanics and Physics of Solids,* 1997; **45**:535–563.

Seagraves A, Radovitzky R. "Advances in cohesive zone modeling of dynamic fracture". *Dynamic Failure of Materials and Structures*. Springer Science and Business Media: Berlin, 2010.

Simone, A. (2004), "Partition of unity-based discontinuous elements for interface phenomena: computational issues". *Commun. Numer. Meth. Engng*., 20: 465–478.

Song J-H, Areias PMA, Belytschko T (2006) ,"A method for dynamic crack and shear band propagation with phantom nodes". *Int J Numer Meth Eng* 67:868–893.

T.P. Fries and T. Belytschko. "The extended/generalized finite element method: An overview of the method and its applications". *Internat. J. Numer. Methods Engrg.*, 84:253 – 304, 2010.

Wriggers P, Zavarise G. "A formulation for frictionless contact problems using a weak form introduced by Nitsche". *Comput. Mech*. 2008; 41(3):407-420.

Xu X, Needleman A. "Numerical simulations of fast crack growth in brittle solids". *Journal of the Mechanics and Physics of Solids* 1994; **42**:1397–1434.

Zavattieri P, Espinosa H. "Grain level model analysis of crack initiation and propagation in brittle materials". *Acta Materialia* 2001; **49**:4291–4311.

Zhengyu (Jenny) Zhang, Glaucio H. Paulino, "Cohesive zone modeling of dynamic failure in homogeneous and functionally graded materials", *International Journal of Plasticity*, Volume 21, Issue 6, June 2005, Pages 1195-1254.

Zhang, Z., Paulino, G. H. and Celes, W. (2007), "Extrinsic cohesive modelling of dynamic fracture and microbranching instability in brittle materials". *Int. J. Numer. Meth. Engng.*, 72: 893–923.